A quinoline-based fluorometric and colorimetric dual-modal pH probe and its application in bioimaging

Qin Zhu[a], Zhao Li[a], Lan Mu[a*], Xi Zeng[a], Carl Redshaw[b], Gang Wei[c*]

[a] Key Laboratory of Macrocyclic and Supramolecular Chemistry of Guizhou Province, Guizhou University, Guiyang 550025, P.R. China

[b] Department of Chemistry, University of Hull, Hull HU6 7RX, U. K

[c] CSIRO Manufacturing Flagship, PO Box 218, NSW 2070, Australia

*Corresponding author. lmu@gzu.edu.cn, Tel.: +86-139-8553-7291; gang.wei@csiro.au, Tel.: +61-2-94137704.

ABSTRACT: The compound (*E*)-8-hydroxyl-2-[(*E*)-2-(2, 4-dihydroxyphenyl)vinyl]-quinoline (**1**) has been developed as a fluorometric and colorimetric dual-modal probe for pH detection in solution and *in vivo*. Remarkable changes in the fluorescence intensity with large Stokes shifts and colorimetric responses were observed as a function of pH. The sensing mechanisms involving protonation and deprotonation processes over the acidic and alkaline pH ranges were confirmed by ^{1}H NMR and IR spectroscopic analysis. Furthermore, the application of probe **1** for the imaging of live PC3 cells was successfully achieved. Test strips based on probe **1** were fabricated, and were found to act as a convenient and efficient pH test kits.

Keywords: Quinoline, pH probe, Fluorometric, Colorimetric, Bioimaging

---

* Corresponding author. Tel.: +86-139-8553-7291. Tel.: +61-2-94137704
E-mail address: lmu@gzu.edu.cn (Lan Mu); gang.wei@csiro.au (Gang Wei).

1. Introduction

pH plays a vital role in cell metabolism processes, including proliferation, apoptosis, enzyme activity and protein degradation [1-5]. Monitoring variations of intracellular pH in living cells is thus of great importance due to its direct link with many common diseases such as cancer, Alzheimer's and many others [6, 7]. Fluorescence spectroscopy and fluorescence imaging techniques have many advantages including high sensitivity, high spatial and temporal resolution and are not destructive to the cells. As such, molecular fluorescent pH probes have become indispensable tools for observing pH changes in cells [8].

Fluorescence pH probes have found wide use in analytical chemistry, bio-analytical chemistry, and cellular biology. Over the past few years, the intelligent design of synthetic methods has led to the development of pH fluorescent probes based on quinoline [9-12], coumarin [12-14], indoles [15-17], dansyl [18], rhodamine [19-23], quaternary ammonium salt [24], naphthalimide [25, 26], benzothiazole [27], cyanine dyes [28, 29]. In particular, pH-sensitive fluorescent probes which operate near neutral pH for intracellular fluorescence imaging have been widely studied [30-36]. Generally, there are two ranges of pH that exists in cells, pH = 6.8 ~ 7.4, as well as the cytoplasm; pH = 4.5 ~ 6.0, known as acidic organelles. For instance, the acidic environments in lysosomes (pH 4.5 ~ 5.5) can facilitate the degradation of proteins in cellular metabolism [37, 38]. Actually, most living species would find it hard to survive under extreme pH conditions, whereas a mass of microorganisms such as "acidophiles" and helicobacter pylori favor such harsh environments [39, 40]. Nevertheless, most of the reported pH-sensitive fluorescent probes work under neutral or slightly acidic conditions, and only a few of them can operate for imaging of living

cells under extreme acidity [8, 14, 16, 17, 27, 41] or over the full-range of pH [42, 43]. Much less attention has been paid to fluorescent probes which are pH-sensitive in the lower pH region (pH < 5) or the higher pH region (pH > 9). This inspired us to develop a highly sensitive pH fluorescent probe for extreme pH ranges.

Herein, we report a quinoline-based fluorometric and colorimetric probe **1** for pH detection in solution and *in vivo* (Scheme 1). As a novel pH-sensitive probe, probe **1** has a large Stokes shift, a good quantum yield, and promising specificity. In particular, it is capable of measurements at extreme pH values, specifically over the two pH ranges 2.2 ~ 4.8 and 10.0 ~ 11.4, respectively. Importantly, the application of probe **1** for the imaging of live PC3 cells was successfully achieved, and we have demonstrated that probe **1** can be used as pH test strips for the instantaneous detection of pH. Additionally, the sensing mechanism of probe **1** had been confirmed by ^{1}H NMR and IR spectroscopic experiments.

Insert Scheme 1 in here

2. Experimental

2.1. Materials and methods

Unless otherwise stated, all reagents were purchased from commercial sources and used without further purification. Tris/HEPES, amino acids and biochemical reagents were purchased from Shanghai Macklin Biochemical Co., Ltd. or Sinopharm Chemical Reagent Co., Ltd. Metal ions were purchased from Aldrich or Alfa Aesar Chemical Co., Ltd. Acetonitrile was purchased from Tianjin Kemiou Chemical Reagent Co., Ltd. Roswell Park Memorial Institute-1640 or from Bengjing Dingguo biological Co., Ltd. Test papers were prepared from filter paper that was cut into 1 cm × 5 cm strips. A test strip was conveniently prepared by dipping into a

solution of probe **1** and then drying in air, and subsequently dipping into an aqueous of Tris-HCl or HEPES-NaOH buffer solution at different pH values.

All fluorescence measurements were acquired by using a Cary Eclipse Fluorescence Spectrometer (Varian) in a 1 cm quartz cell. UV-Vis absorption spectra were conducted on a UV-1800 spectrophotometer (Shimadzu) in a 1 cm quartz cell. ^{1}H NMR spectra were recorded on a WNMR-I 500 MHz NMR (at the Wuhan Institute of Physics and Mathematics, Chinese Academy of Sciences) and using TMS as an internal standard at room temperature. IR spectra were obtained using a Vertex 70 FT-IR spectrometer (Bruker). Fluorescence imaging was conducted on a Ti (Nikon) fluorescent inverted phase contrast microscope. Various pH solutions were measured by using a pH meter (Orion). Probe **1** (*E*)-8-hydroxyl-2-[(*E*)-2-(2,4-dihydroxyphenyl)vinyl]-quinoline was prepared following our previously reported procedure [44].

2.2 Analytical procedure

For absorption or fluorescence measurements, probe **1** was dissolved in CH$_3$CN to obtain stock solutions (1 mM). The stock solutions of metal ions (20 mM) were prepared in water by dissolving a pre-determined amount of their perchlorate salt. Stock solutions of bioactive species (50 mM) such as amino acids, proteins, reactive oxygen species and reducing agents were prepared in water.

The pH-dependent spectral characteristics of probe **1** (10 μM) were evaluated in a Tris buffer or HEPES buffer solution with CH$_3$CN as a co-solvent. Probe **1** (0.1 mM) was diluted by CH$_3$CN and Tris-HCl (50 mM) buffers with pH from 1.6 to 5.0, as well as by CH$_3$CN and HEPES-NaOH (50 mM) buffers with pH from 6.0 to 11.4. All experiments were performed in CH$_3$CN/Tris or HEPES (v/v, 3/2) buffer aqueous solution and the pH value was confirmed by pH meter.

The buffered solutions at various pH values were modulated by mixing Tris with HCl (pH = 1.6 ~ 5.0) and HEPES with NaOH (pH = 6.0 ~ 11.4), respectively. The preparation of Tris-HCl buffer solutions involved weighing 6.057g of Tris, dissolving it in ultrapure water, diluting to 1L and formulating as a 50 mM solution. Solutions of various pH values were obtained by adding the appropriate amount of HCl solution to 50 mM Tris solution and monitoring with a pH meter. When the pH value is smaller, the stronger the acidity, and the addition amount of Tris is limited; the Tris-HCl buffer solutions can match to 1.6 ~ 5.0. Given HEPES is a kind of zwitterionic organic chemistry buffer, NaOH solution was added to HEPES solution to adjust the pH value over the range 6.0 ~ 11.4. The preparation method for the HEPES-NaOH buffer solution is the same as that for the Tris-HCl buffered solution.

2.3 Cell culture

The Roswell Park Memorial Institute-1640 (RPMI-1640) supplemented with 10 % fetal bovine serum, 100 μg/mL penicillin and 100 μg/mL streptomycin were employed to culture the human prostate cancer cells (PC3). These cells were grown in a culture dish at 37 ºC and in the presence of 5 % CO_2. One day before imaging, the cells were seeded in a 12-well culture dish, after incubation for 24 h, then incubated with probe **1** (10 μM) in an RPMI-1640 culture medium at 37 ºC for 1h. After washing with fresh culture medium three times, the cells were then incubated with 20 mM Tris-HCl or HEPES-NaOH buffer for 15 min at various pH values.

3. Results and discussion

*3.1 Spectra characteristics and optical responses to pH of probe **1***

The pH response properties of probe **1** were primarily investigated in a CH_3CN/buffered solution at various pH values (pH ranged from 2.0 to 11.4). The results with respect to the pH response properties are depicted in Fig. S1. Probe **1**

exhibited relatively weak fluorescence when the pH values ranged from 5.0 to 10.0 when excited at λ_{ex} = 440 nm. Interestingly, a sharp enhancement in fluorescence intensity at 550 nm appeared when the pH was decreased from 4.0 to 2.0, and another enhancement in fluorescence intensity at 580 nm appeared when the pH was raised from 10.0 to 11.4. Similarly, probe **1** exhibits almost no absorbance at about 430 nm under neutral conditions, but when the pH ranged from 4.0 ~ 2.0 or 10.0 ~ 11.4, a remarkable absorbance enhancement was observed (Fig. S1b). The optical responses to pH of probe **1** as a function of pH displayed a reversible ''on-off-on'' optical switch type mode.

3.2 UV-Vis absorption properties of probe 1

The pH-dependent optical response properties of probe **1** (10 μM, CH₃CN/Tris or HEPES, v/v, 3/2) were further investigated in detail. Under acidic conditions, as the pH value decreased from 5.0 to 1.6, the absorption band of probe **1** at around 430 nm gradually reduced, whereas a new peak emerged at 360 nm. An obvious blue shift (~ 70 nm) in the UV-Vis absorption spectra and a well-defined isobestic point at about 385 nm can be observed (Fig. 1). The absorbance of probe **1** at around 430 nm enhanced when the pH value decreased from 5.0 to 1.6 as evidenced by an absorbance titration (Fig. 1, inset). Good linearity (R^2 = 0.9923) between the absorbance at 430 nm and the pH value over the range 2.2 to 4.6 was obtained (Fig. S4). These remarkable changes in the absorption spectra resulted in an obvious colour change of the solution of probe **1** from deep yellow green to light yellow green upon increasing the pH from 2.2 to 4.6, and finally it became colourless when the pH value was greater than 4.6 under visible light (Fig. S5).

Insert Fig. 1 in here

The band of probe **1** centred at around 360 nm gradually enhanced when the pH increased from barely acidic to alkaline (Fig. S6). Good linearity ($R^2 = 0.9847$) between the absorbance at 360 nm and the pH over the range 5.0 to 10.0 was observed as evidenced by an absorbance titration (Fig. S7). However, under alkaline conditions, as the pH increased from 10.0 to 11.4, the absorption band centered at 430 nm gradually increased, while the band at 360 nm simultaneously decreased. A gradual red shift (~ 70 nm) can be observed, as well as a well-defined isobestic point at 390 nm (Fig. 2). Good linearity ($R^2 = 0.9923$) between the absorbance at 430 nm and pH over the range 10.0 to 11.4 was evident (Fig. S8). The colour of the solution of probe **1** changed from light orange to orange/red upon increasing the pH from 10.0 to 11.4 under visible light (Fig. S9). Given the above results, it is clear that probe **1** is capable of measuring extreme pH values over the three pH ranges of 2.2 ~ 4.6, 5.0 ~ 10.0 and 10.0 ~ 11.4, respectively. The probe **1** undergoes distinct colour changes on varying the pH value, which suggests it can serve as a "naked-eye" indicator of pH.

Insert Fig. 2 in here

*3.3 Fluorescence properties of probe **1***

The pH-dependent fluorescence characteristics of probe **1** (10 μM) were also evaluated. Over the pH range 5.0 to 8.0, probe **1** exhibits a relative weak fluorescence emission peak centered at around 550 nm with excitation at 440 nm. As shown in Fig. 3, on decreasing the pH value from 5.0 to 1.6, an evident enhancement of the fluorescent emission at 550 nm was observed with the excitation wavelength of 440 nm. In comparison, when an excitation wavelength of 360 nm was used, the emission band at about 550 nm decreased and a striking new peak emerged at 480 nm, revealing a large blue shift of 70 nm (Fig. S10). Good linearity ($R^2 = 0.9951$) between the fluorescent intensity and pH value was obtained according to fluorescence titration

experiments (Fig. S11). The colour of the probe **1** solution changed from yellow/green to green on increasing the pH from 2.2 to 3.6, and finally it became blue and dark blue when the pH exceeded 3.6 under ultraviolet light (Fig. S12).

Insert Fig. 3 in here

Additionally, the fluorescence changes under alkaline conditions were also examined. On increasing the pH from 10.0 to 11.4, a new fluorescence peak emerges with the fluorescent intensity gradually enhanced at 580 nm, which represents a 30 nm red-shift as compared to that at pH 4.6 (Fig. 4). Good linearity (R^2 = 0.9995) between fluorescent intensity and pH over the range 10.0 to 11.4 was observed by fluorescence titration experiments (Fig. S13). The colour of the probe **1** solution changed from light orange to orange/red on increasing the pH from 10.0 to 11.4 under ultraviolet light (Fig. S14). A plot of the fluorescence intensity as a function of pH using the Henderson-Hasselbalch equation [45] afforded a calculated pK_a value of 3.32 (Fig. 3, inset) and 10.75 (Fig. 4, inset), respectively. Fluorescence quantum yield and photochemical properties measurements for probe **1** at pH 2.2, 4.6, 10 and 11.4 are given in Table S1. Notably, probe **1** has large Stokes shifts ($\Delta\lambda$ = 110 nm at pH 2.2 ~ 4.6, $\Delta\lambda$ = 140 nm at pH 10.0 ~ 11.4). We note that the detection sensitivity can be improved by the presence of large Stokes shifts because of reduced self-quenching and minimized measurement errors. As a result, probe **1** is capable of measuring extreme pH values over the two pH ranges 2.2 ~ 4.6 and 10.0 ~ 11.4, respectively.

Insert Fig. 4 in here

3.4 Stability, reversibility and selectivity of probe **1**

In order to determine the impact of time on this detection process, an estimation of the time-dependent fluorescence spectral changes of probe **1** at different pH values was carried out. As shown in Fig. S15, the fluorescence emission enhanced

immediately and the fluorescence intensity remained stable over long periods. The reversibility of a pH probe is also of great importance to its practical application, so the pH value was modulated repeatedly between 2.0 and 7.0, 7.0 and 11.4 several times, and the corresponding emissions were monitored. As shown in Fig. 5, when solutions containing probe **1** were changed to low or high pH, no obvious variation in the fluorescence intensity of probe **1** was observed after six cycles. This circulation could be repeated for at least six times, and such a reversible pH response indicated that it will be a benefit for fluorescent intracellular pH imaging. The fluorescence responses of probe **1** as a function of pH displayed a reversible ''on-off-on'' switch type mode: the fluorescence "on" state under acidic conditions is due to the protonation of the nitrogen atom; on the other hand, the fluorescence "on" state under alkaline conditions is attributed to the loss of a proton from the phenolic hydroxyl group; the fluorescence "off" state is adopted under neutral conditions [46].

Insert Fig. 5 in here

The selectivity of probe **1** for preferential binding to H^+ over other potential competing ions was also investigated under acidic and alkaline conditions. As shown in Fig. S16, no noticeable change was observed in the absorbance and fluorescence intensity of probe **1** (10 μM) at pH 3.6 and pH 10.6 in the presence of various metal ions, such as Na^+, K^+, Mg^{2+}, Ca^{2+}, Ba^{2+}, Zn^{2+}, Pb^{2+}, Ni^{2+}, Hg^{2+}, Cu^{2+}, Ag^+, and Fe^{3+}. Moreover, some other bioactive species such as Cys, Lys, Tyr, Trp, Arg, Glu, BSA, BHb, and D-levulose were also evaluated, and no obvious changes were observed. These results revealed that probe **1** exhibited an excellent selectivity response to pH in the presence of a number of background metal ions and bioactive species as described above. Moreover, high concentrations of Na^+, K^+, Mg^{2+} and Ca^{2+}, which are abundant in cells, as well as heavy and transition metal ions, such as Ba^{2+}, Zn^{2+}, Pb^{2+}, Ag^+, Fe^{3+},

9

Ni^{2+}, Hg^{2+}, Cu^{2+}, and some biologically important amino acids had no effect on the pH response of the probe at the different pH values employed herein. These results suggest that probe **1** might be a suitable candidate as a staining agent for fluorescent intracellular pH imaging.

3.5 Application of pH test paper

In order to employ the detection in a feasible method, a test strip was conveniently prepared by dip coating a solution of probe **1** and then drying it in air. When the test papers were immersed in an aqueous of Tris-HCl or HEPES-NaOH buffer solution at different pH values, the colour of the test strips of probe **1** changed immediately. Under visible light, the yellow/green of the test papers gradually faded away as the pH increased from 2.2 to 4.6; and the orange/red was enhanced when the pH increased from 10.2 to 11.4 (Fig. 6a). Under ultraviolet light, the test papers undergo a much more obvious colour change, displaying yellow/green, green and blue fluorescence on increasing the pH from 2.2 to 4.6; and the orange/red enhanced when the pH increased from 10.2 to 11.4 (Fig. 6b). Therefore, the test strips could conveniently detect pH over a wide pH range.

Insert Fig. 6 in here

*3.6 Fluorescence imaging of probe **1** in living PC3 cells*

Encouraged by the desirable pH-dependent spectral properties of the probe **1**, its potential for monitoring pH changes in living cells was then examined. PC3 cells were incubated with probe **1** (10 μM) for 1 h. After washing with fresh RPMI-1640 culture medium for three times, the cells were then incubating with 50 mM Tris-HCl buffer or HEPES-NaOH buffer at various pH values for 15 min. Prior to imaging, cells were washed with fresh RPMI-1640 culture medium three times. Fluorescence images were acquired on a fluorescence microscopy in the green channel ($\lambda_{ex} = 450 \sim$

490 nm) or in the red channel (λ_{ex} = 510 ~ 550 nm). As shown in Fig. 7, the cells exhibited green fluorescence from the green channel, and the intensity of the green fluorescence gradually weakened when the pH changed from 2.0 to 4.0 (Fig. 7a and 7b). Furthermore, the cells showed red fluorescence from the red channel, and the intensity of the red fluorescence gradually increased when the pH changed from 10.0 to 11.4 (Fig. 7e and 7f); no fluorescence was exhibited at pH 7.0 (Fig. 7i). The cell imaging changes *versus* the pH values are consistent with the previous spectral properties, and indicate that the probe has good membrane permeability, clear cellular location and low cytotoxicity for measuring extreme ranges of intracellular pH.

Insert Fig. 7 in here

3.7 The mechanism of pH detection

In order to obtain more detailed information on the sensing mechanism, ^{1}H NMR titrations of probe **1** (5 mM) under acidic and alkaline conditions were performed in CD$_3$CN/D$_2$O (3/1, v/v). As shown in Fig. 8a, upon addition of DCl, the chemical shifts of H5 ~ H10 in probe **1** exhibited a distinct downfield shift by $\Delta\delta$ 0.194 ~ 0.478 ppm. The large change of proton resonance revealed the protonation of the nitrogen atom on the 8-hydroxyquinoline, which enhanced the electron-withdrawing effect, and decreased the electron density of the aromatic ring, leading to the downfield shift of the proton signals. On the other hand, when NaOD was added to the solution of probe **1** (Fig. 8b), all the proton signals of the conjugation system clearly shift upfield (Table S2), with H1 and H2 showing an especially large shift $\Delta\delta$ (H1) = 0.144 ppm and $\Delta\delta$ (H2) = 0.135 ppm, which indicated that the deprotonation of the phenolic hydroxy group of probe **1** enhanced the electron-donating and p-π conjugate effect, increased the electron density of the aromatic ring, and led to the upfield shift of the

proton signals. Therefore, the probe **1** exhibits multi-colours under acidic and alkaline conditions, which allows for the distinction of pH values over a wide range.

Insert Fig. 8 in here

The IR spectra of probe **1**, probe **1**·HCl and probe **1**·NaOH were measured. There were obvious differences in the spectra, namely the peak at 3390 cm^{-1} was attributed to the stretching vibration of the phenolic hydroxy group on probe **1** due to the formation the hydrogen-bonding. The peak at 1450 cm^{-1} was attributed to the stretching vibration of the benzene ring and 1600 cm^{-1} was attributed to the stretching vibration of C=C, which changed dramatically on adding HCl due to the protonation of the nitrogen atom and enhancement of the electronic withdrawing effect (Fig. S17a). The peak at 3390 cm^{-1} of the phenolic hydroxy group of probe **1** decreased remarkably because of weakening of the hydrogen-bonding by the deprotonation of the phenolic hydroxy group. Meanwhile, the peak at 1450 cm^{-1} and 1600 cm^{-1} changed on adding NaOH due to p-π conjugation and the improvement of the skeleton vibrations of the benzene ring (Fig. S17b). Thus, the changes of the IR spectra of probe **1** on adding HCl and NaOH are consistent with the results from the ^{1}H NMR spectroscopic titrations. According to the above experiments, a pH modulated switching of probe **1** *versus* pH is proposed as shown in Scheme 2.

Insert Scheme 2 in here

4. Conclusions

In summary, we have described a novel quinoline-based pH-sensitive probe **1**, which could respond to pH via different fluorescence and absorption changes based on a protonation and deprotonation mechanism. Probe **1** could respond to a broad pH range from 2.0 to 11.4 via different fluorescence emissions (green/blue at pH 2.0 ~ 5.0, quenching at pH 5.0 ~ 10.0, and orange/red at pH 10.0 ~ 11.4). Common

potentially competing ions and bioactive species did not cause any obvious interference for the pH sensing process. Probe **1** has advantages including responding to pH via different fluorescence emissions, good reversibility, excellent anti-interference and sensing over a wide pH range, all of which make it behave as an excellent pH probe compared with many previous pH probes reported in terms of selectivity, sensitivity, pH detection range and applications (Table S3). In particular, the application of probe **1** for the pH detection in PC3 cells was successfully achieved, proving that it can reveal intracellular pH fluctuations. This study may provide a promising candidate for intracellular pH detection application in both chemical and biological fields.

Acknowledgments

Appendix A. Supplementary data

References

[1] V.A. Golovina, M.P. Blaustein, Spatially and functionally distinct Ca^{2+} stores in sarcoplasmic and endoplasmic reticulum, Science. 275 (1997) 1643-1648.

[2] A. Ishaque, M. Al-Rubeai, Use of intracellular pH and annexin-V flow cytometric assays to monitor apoptosis and its suppression by bcl-2 over-expression in hybridoma cell culture, J. Immunol. Methods. 221 (1998) 43-57.

[3] R.G. W. Anderson, L. Orci, A view of acidic intracellular compartments, J. Cell Biol. 106 (1988) 539-543.

[4] R.J. Gillies, N. Raghunand, M.L. Garcia-Martin, R.A. Gatenby, A review of pH measurement methods and applications in cancers, Ieee Eng. Med. Biol. 23 (2004) 57-64.

[5] H. Izumi, T. Torigoe, H. Ishiguchi, H. Uramoto, Y. Yoshida, M. Tanabe, T. Ise, T. Murakami, T. Yoshida, M. Nomoto, K. Kohno, Cellular pH regulators: potentially promising molecular targets for cancer chemotherapy, Cancer Treat. Rev. 29 (2003) 541-549.

[6] V. Vingtdeux, M. Hamdane, S. Bégard, A. Loyens, A. Delacourte, J.C. Beauvillain, L. Buée, P. Marambaud, N. Sergeant, Intracellular pH regulates amyloid precursor protein intracellular domain accumulation, Neurobiol. Dis. 25 (2007) 686-696.

[7] B.Y. Fang, D.J. Wang, M.F. Huang, G.H. Yu, H. Li, Hypothesis on the relationship between the change in intracellular pH and incidence of sporadic Alzheimer's disease or vascular dementia, Int. J. Neurosci. 120 (2010) 591-595.

[8] M.H. Su, Y. Liu, H.M. Ma, Q.L. Ma, Z.H. Wang, J.L. Yang, M.X. Wang, 1,9-Dihydro-3-phenyl-4H-pyrazolo[3,4-b]quinolin-4-one, a novel fluorescent probe for extreme pH measurement, Chem. Commun. (2001) 960-961.

[9] X.T. Li, M. Zhang, H.P. Liang, Z.W. Huang, J. Tang, Z. Chen, L.T. Yang, L.J. Ma, Y.H. Wang, B.P. Xu, 4-(8-Quinolyl)amino-7-nitro-2,1,3-benzoxadiazole as a new selective and sensitive fluorescent and colorimetric pH probe with dual-responsive ranges in aqueous solutions, Spectrochim Acta A. 153 (2016) 517-521.

[10] S. Mukherjee, A.K. Paul, K.K. Rajak, H. Stoeckli-Evans, ICT based ratiometric fluorescent pH sensing using quinoline hydrazones, Sens. Actuators B. 203 (2014) 150-156.

[11] G.P. Li, D.J. Zhu, L. Xue, H. Jiang, Quinoline-Based Fluorescent Probe for Ratiometric Detection of Lysosomal pH, Org. Lett. 15 (2013) 5020-5023.

[12] S.S. Zhu, W.Y. Lin, L. Yuan, Development of a ratiometric fluorescent pH probe for cell imaging based on a coumarine-quinoline platform, Dyes Pigm. 99 (2013) 465-471.

[13] X.D. Liu, Y. Xu, R. Sun, Y.J. Xu, J.M. Lu, J.F. Ge, A coumarin-indole-based near-infrared ratiometric pH probe for intracellular fluorescence imaging, Analyst. 138 (2013) 6542-6550.

[14] Y. Xu, Z. Jiang, Y. Xiao, F.Z. Bi, J.Y. Miao, B.X. Zhao, A new fluorescent pH probe for extremely acidic conditions, Anal. Chim. Acta. 820 (2014) 146-151.

[15] W.F. Niu, M. Nan, L. Fan, M.S. Wong, S.M. Shuang, C. Dong, A novel pH fluorescent probe based on indocyanine for imaging of living cells, Dyes Pigm. 126 (2016) 224-231.

[16] L. Fan, S.Q. Gao, Z.B. Li, W.F. Niu, W.J. Zhang, S.M. Shuang, C. Dong, An indole-carbazole-based ratiometric emission pH fluorescent probe for imaging extreme acidity, Sens. Actuators B. 221 (2015) 1069-1076.

[17] W.F. Niu, L. Fan, M. Nan, Z.B. Li, D.T. Lu, M.S. Wong, S.M. Shuang, C. Dong, Ratiometric Emission Fluorescent pH Probe for Imaging of Living Cells in Extreme Acidity, Anal. Chem. 87 (2015) 2788-2793.

[18] M. Zhang, S.Y. Zheng, L.G. Ma, M.L. Zhao, L.F. Deng, L.T. Yang, L.J. Ma, Dansyl-8-aminoquinoline as a sensitive pH fluorescent probe with dual-responsive ranges in aqueous solutions, Spectrochim Acta A. 124 (2014) 682-686.

[19] W.L. Czaplyski, G.E. Purnell, C.A. Roberts, R.M. Allred, E.J. Harbron, Substituent effects on the turn-on kinetics of rhodamine-based fluorescent pH probes, Org. Biomol. Chem. 12 (2014) 526-533.

[20] G.J. Song, S.Y. Bai, X. Dai, X.Q. Cao, B.X. Zhao, A ratiometric lysosomal pH probe based on the imidazo[1,5-a]pyridine-rhodamine FRET and ICT system, RSC Adv. 6 (2016) 41317-41322.

[21] L.J. Liu, P. Guo, L. Chai, Q. Shi, B.H. Xu, J.P. Yuan, X.G. Wang, X.F. Shi, W.Q. Zhang, Fluorescent and colorimetric detection of pH by a rhodamine-based probe, Sens. Actuators B. 194 (2014) 498-502.

[22] P.Y. Ma, F.H. Liang, D. Wang, Q.Q. Yang, Z.Q. Yang, D.J. Gao, Y. Yu, D.Q. Song, X.H. Wang, A novel fluorescence and surface-enhanced Raman scattering dual-signal probe for pH sensing based on Rhodamine derivative, Dyes Pigm. 122 (2015) 224-230.

[23] F.H. Liang, D. Wang, P.Y. Ma, X.H. Wang, D.Q. Song, Y. Yu, A Highly Selective and Sensitive Ratiometric Fluorescent Probe for pH Measurement Based on Fluorescence Resonance Energy Transfer, Chem. Res. Chin. Univ. 31 (2015) 724-729.

[24] X.X. Zhao, D. Ge, X. Dai, W.L. Wu, J.Y. Miao, B.X. Zhao, A water-soluble pH fluorescence probe based on quaternary ammonium salt for bioanalytical applications, Spectrochim Acta A. 151 (2015) 218-224.

[25] J. Zhou, C.L. Fang, T.J. Chang, X.J. Liu, D.H. Shangguan, A pH sensitive ratiometric fluorophore and its application for monitoring the intracellular and extracellular pHs simultaneously, J. Mater. Chem. B. 1 (2013) 661-667.

[26] J.L. Hu, F. Wu, S. Feng, J.H. Xu, Z.G. Xu, Y.Q. Chen, T. Tang, X.C. Weng, X. Zhou, A convenient ratiomeric pH probe and its application for monitoring pH change in living cells, Sens. Actuators B. 196 (2014) 194-202.

[27] J.B. Chao, Y.H. Liu, J.Y. Sun, L. Fan, Y.B. Zhang, H.H. Tong, Z.Q. Li, A ratiometric pH probe for intracellular pH imaging. Sens. Actuators B. 221 (2015) 427-433.

[28] J.T. Miao, C. Fan, X.Y. Shi, R. Sun, Y.J. Xu, J.F. Ge, Colorimetric and ratiometric pH responses by the rotonation of phenolate within hemicyanine, Analyst. 139 (2014) 6290-6297.

[29] L.T. Zeng, N. Fan, J.Y. Zha, X.C. Hu, B.Q. Fu, C.Q. Qin, L. Wang, Novel and photostable pH probe for selectively taining nuclei in living cells. Analyst. 138 (2013) 7083-7086.

[30] W.J. Zhang, L. Fan, Z.B. Li, T. Ou, H.J. Zhai, J. Yang, C. Dong, S.M. Shuang, Thiazole-based ratiometric fluorescence pH probe with large Stokes shift for intracellular imaging, Sens. Actuators B. 233 (2016) 566-573.

[31] J.T. Zhang, M. Yang, W. Mazi, K. Adhikari, M.X. Fang, F. Xie, L. Valenzano, A. Tiwari, F.T. Luo, H.Y. Liu, Unusual Fluorescent Responses of Morpholine-Functionalized Fluorescent Probes to pH via Manipulation of BODIPY's HOMO and LUMO Energy Orbitals for Intracellular pH Detection, ACS Sens. 1 (2016) 158-165.

[32] J.T. Zhang, M. Yang, C. Li, N. Dorh, F. Xie, F.T. Luo, A. Tiwari, H.Y. Liu, Near-infrared fluorescent probes based on piperazine-functionalized BODIPY dyes for sensitive detection of lysosomal pH, J. Mater. Chem. B. 3 (2015) 2173-2184.

[33] B.L. Dong, X.Z. Song, C. Wang, X.Q. Kong, Y.H. Tang, W.Y. Lin, Dual Site-Controlled and Lysosome-Targeted Intramolecular Charge Transfer-Photoinduced Electron Transfer-Fluorescence Resonance Energy Transfer Fluorescent Probe for Monitoring pH Changes in Living Cells, Anal. Chem. 88 (2016) 4085-4091.

[34] D.C. Xiang, Q.H. Meng, H. Liu, M.B. Lan, G. Wei, The study of a curcumin-resembling molecular probe for the pH-responsive fluorometric assay and application in cell imaging, Talanta. 146 (2016) 851-856.

[35] Q.Q. Zhang, M. Zhou, A profluorescent ratiometric probe for intracellular pH imaging, Talanta. 131 (2015) 666-671.

[36] X.L. Shi, G.J. Mao, X.B. Zhang, H.W. Liu, Y.J. Gong, Y.X. Wu, L.Y. Zhou, J. Zhang, W.H. Tan, Rhodamine-based fluorescent probe for direct bio-imaging of lysosomal pH changes, Talanta. 130 (2014) 356-362.

[37] H.S. Lv, S.Y. Huan, Y. Xu, X. Dai, J.Y. Miao, B.X. Zhao, A new fluorescent pH probe for imaging lysosomes in living cells, Bioorg, Med. Chem. Lett. 24 (2014) 535-538.

[38] K.K. Yu, K. Li, J.T. Hou, H.H. Qin, Y.M. Xie, C.H. Qiana, X.Q. Yu, Rhodamine-based lysosome-targeted fluorescence probes: high pH sensitivity and their imaging application in living cells, RSC Adv. 4 (2014) 33975-33980.

[39] T.A. Krulwich, G. Sachs, E. Padan, Molecular aspects of bacterial pH sensing and homeostasis, Nat. Rev. Microbiol. 9 (2011) 330-343.

[40] E. Bignell, The molecular basis of pH sensing, signaling, and homeostasis in fungi, Adv. Appl. Microbiol. 79 (2012) 1-18.

[41] X. Zhang, S.Y. Jing, S.Y. Huang, X.W. Zhou, J.M. Bai, B.X. Zhao, New fluorescent pH probes for acid conditions, Sens. Actuators B. 206 (2015) 663-670.

[42] Z.Q. Ma, L. Hu, C. Zhong, H. Zhang, B.F. Liu, Z.H. Liu, A dual-mechanism strategy to design a wide-range pH probe with multicolor fluorescence, Sens. Actuators B. 219 (2015) 179-184.

[43] S. Chen, Y. Hong, Y. Liu, J. Liu, C.W.T. Leung, M. Li, R.T.K. Kwok, E. Zhao, J.W.Y. Lam, Y. Yu, B.Z. Tang, Full-Range Intracellular pH Sensing by an Aggregation-Induced Emission-Active Two-Channel Ratiometric Fluorogen, J. Am. Chem. Soc. 135 (2013) 4926-4929.

[44] Y.H. Zhao, X. Zeng, L. Mu, J. Li, C. Redshaw, G. Wei, A Reversible and Visible Colorimetric/Fluorescent Chemosensor for Al^{3+} and F^- ions with a Large Stoke's Shift, Sens. Actuators B. 204 (2014) 450-458.

[45] R.A. Bissell, A.P. de Silva, H.Q.N. Gunaratne, P.L.M. Lynch, G.E.M. Maguire, K.R.A.S. Sandanayake, Molecular Fluorescent Signalling with 'Fluor-Spacer-Receptor' Systems: Approaches to Sensing and Switching Devices via Supramolecular Photophysics, Chem. Soc. Rev. 21 (1992) 187-195.

[46] K. Sadhu, S. Mizukami, A. Yoshimura, K. Kikuchi, pH Induced dual "OFF-ON-OFF" switch: influence of a suitably placed carboxylic acid, Org. Biomol. Chem. 11 (2013) 563-568.
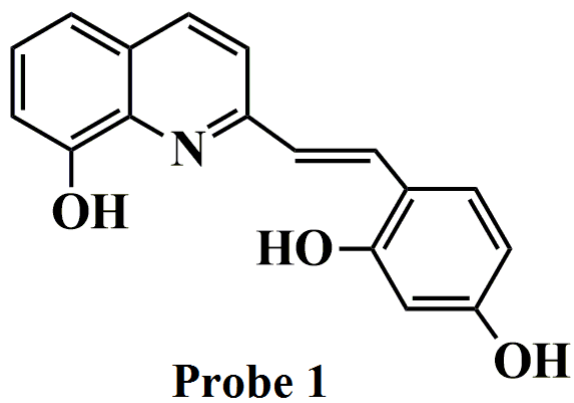
Probe 1

Scheme 1 The structure of probe **1**
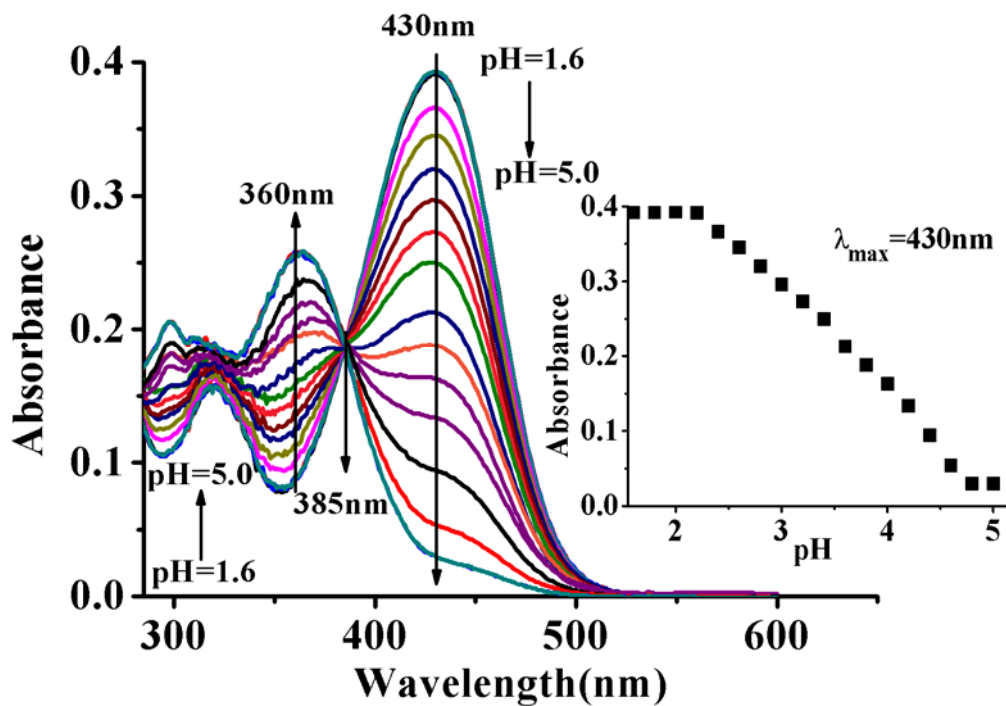
Fig. 1 Absorption spectra of probe **1** (10 μM) in CH₃CN/Tris (v/v, 3/2) buffer solution with pH increase from 1.6 to 5.0, inset shows the changes of maximum absorption at 430 nm on increasing the pH value.
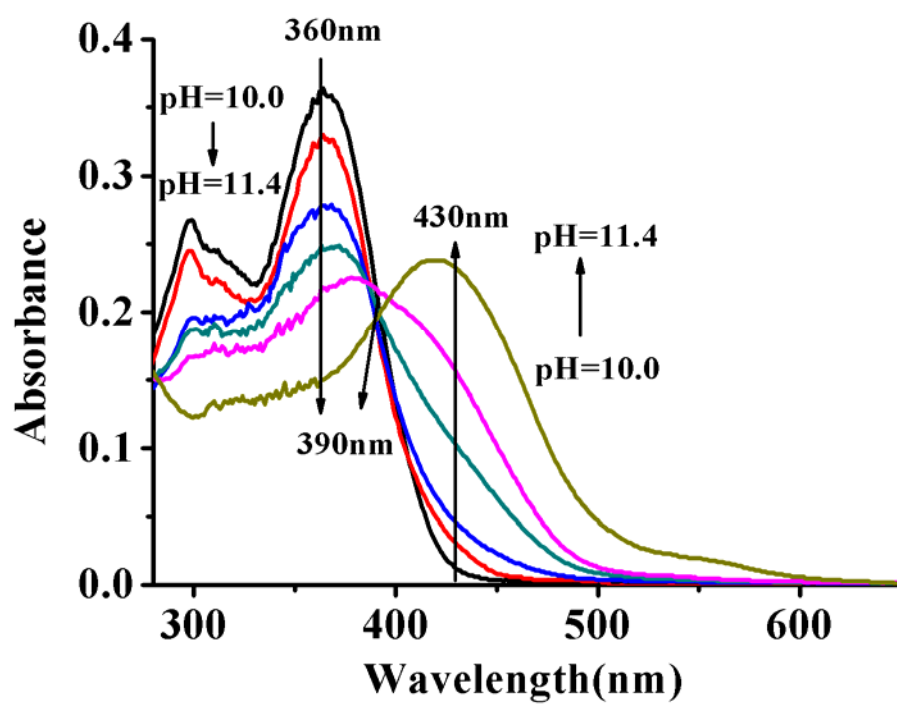
Fig. 2 Absorption spectra of probe **1** (10 μM) in CH₃CN/HEPES (v/v, 3/2) buffer solution on increase of pH from 10.0 to 11.4.
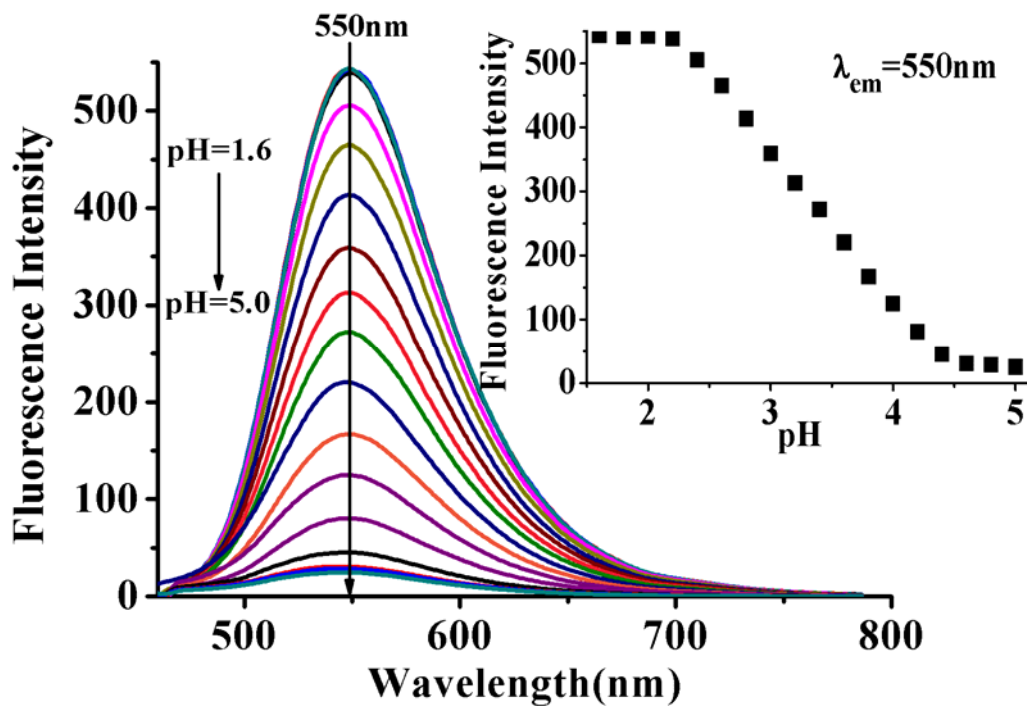
Fig. 3 Fluorescence spectra of probe **1** (10 μM) in CH$_3$CN/Tris (v/v, 3/2) buffer solution on decreasing the pH from 5.0 to 1.6, inset shows a pH-dependent plot of the emission at 550 nm. λ_{ex} = 440 nm.
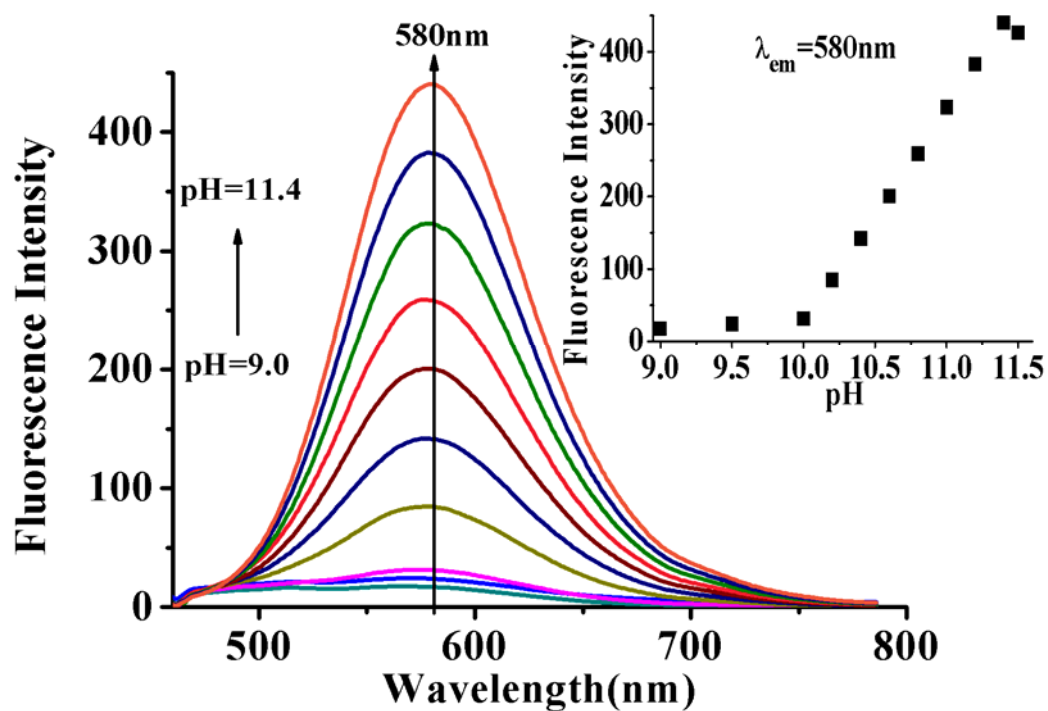
Fig. 4 Fluorescence spectra of probe **1** (10 μM) in CH$_3$CN/HEPES (v/v, 3/2) buffer solution on increasing the pH from 9.0 to 11.4, inset shows a pH-dependent plot of the emission at 580 nm. λ_{ex} = 440 nm.
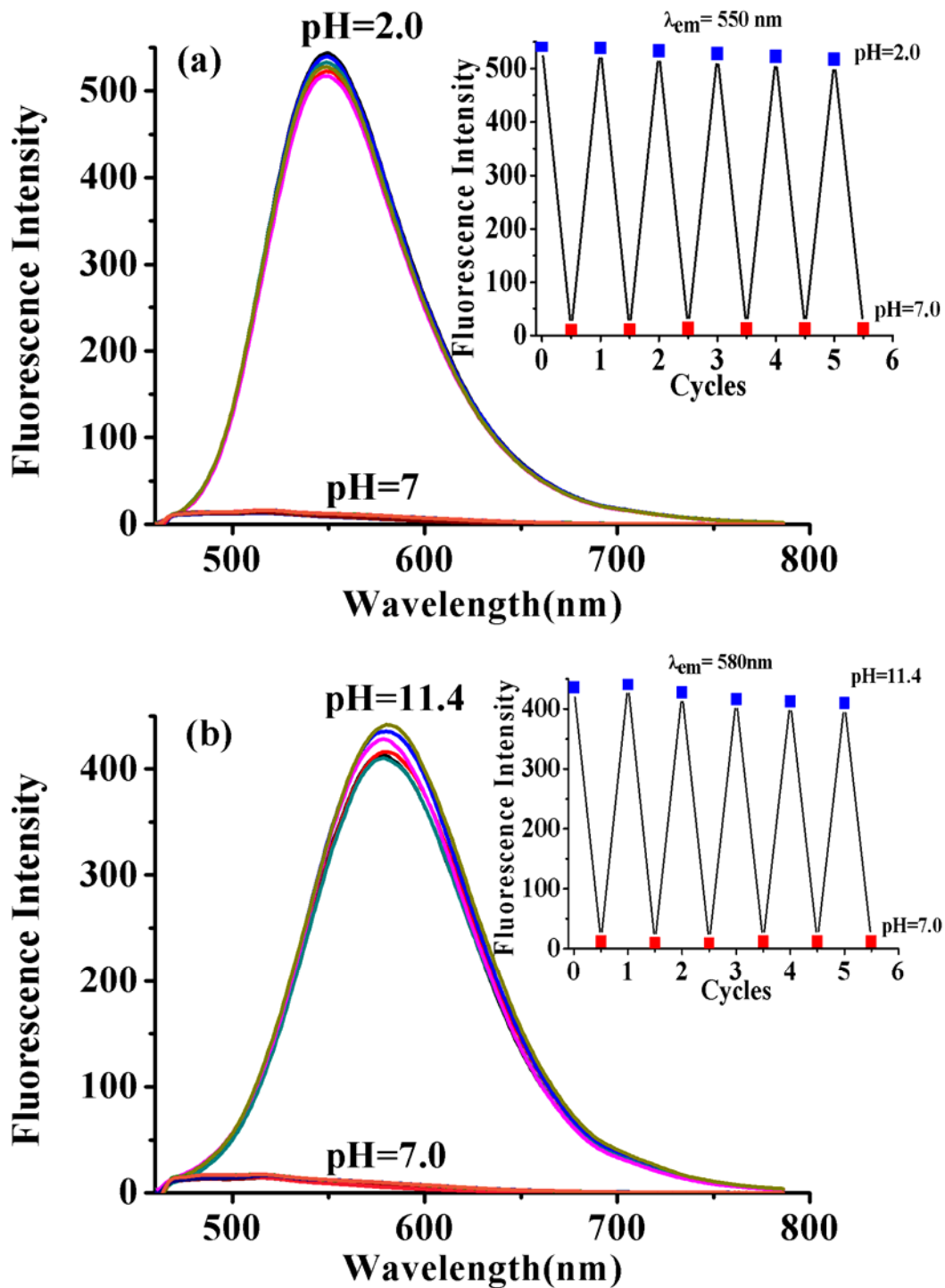
Fig. 5 The pH reversibility of probe **1** (10 μM): (**a**) in CH$_3$CN/Tris (3/2, v/v) buffer

solution with pH 2.0 ~ 7.0; (**b**) in CH$_3$CN/HEPES (3/2, v/v) with pH 7.0 ~ 11.4.
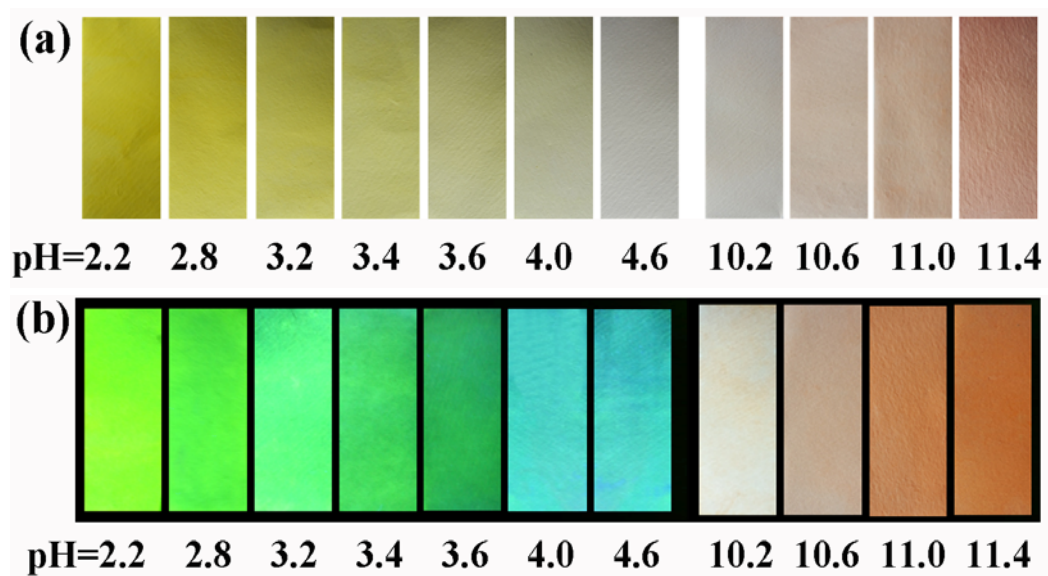
Fig. 6 Colour changes of test papers based on probe **1** at different pH values. **(a)**: under visible light; **(b)**: under 360 nm UV light.
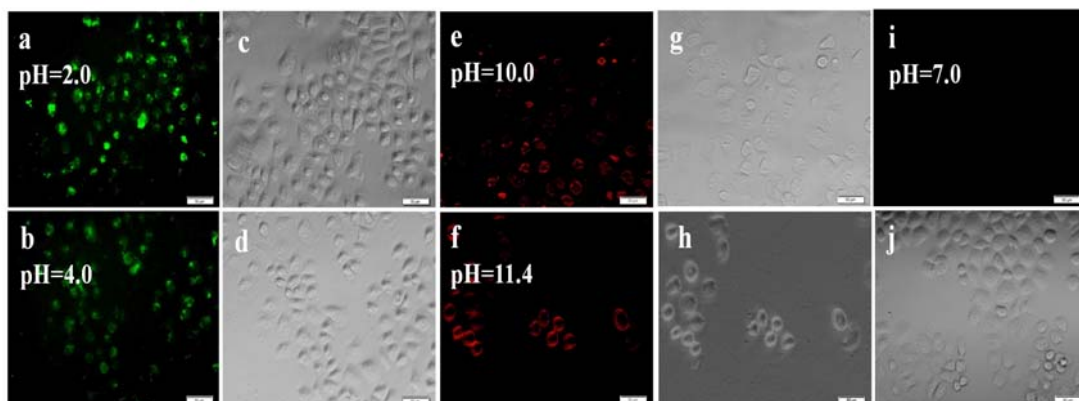
Fig. 7 Fluorescence microscopy analysis of PC3 cells in various pH buffers. PC3 cells incubated with probe **1** (10 μM) for 1 h and then immersed with 50 mM Tris-HCl buffer or HEPES-NaOH buffer for 15 min at pH 2.0 (**a**, **c**: brightfield image); pH 4.0 (**b**, **d**: brightfield image); pH 7.0 (**i**, **j**: brightfield image); pH 10.0 (**e**, **g**: brightfield image), and pH 11.4 (**f**, **h**: brightfield image), respectively.
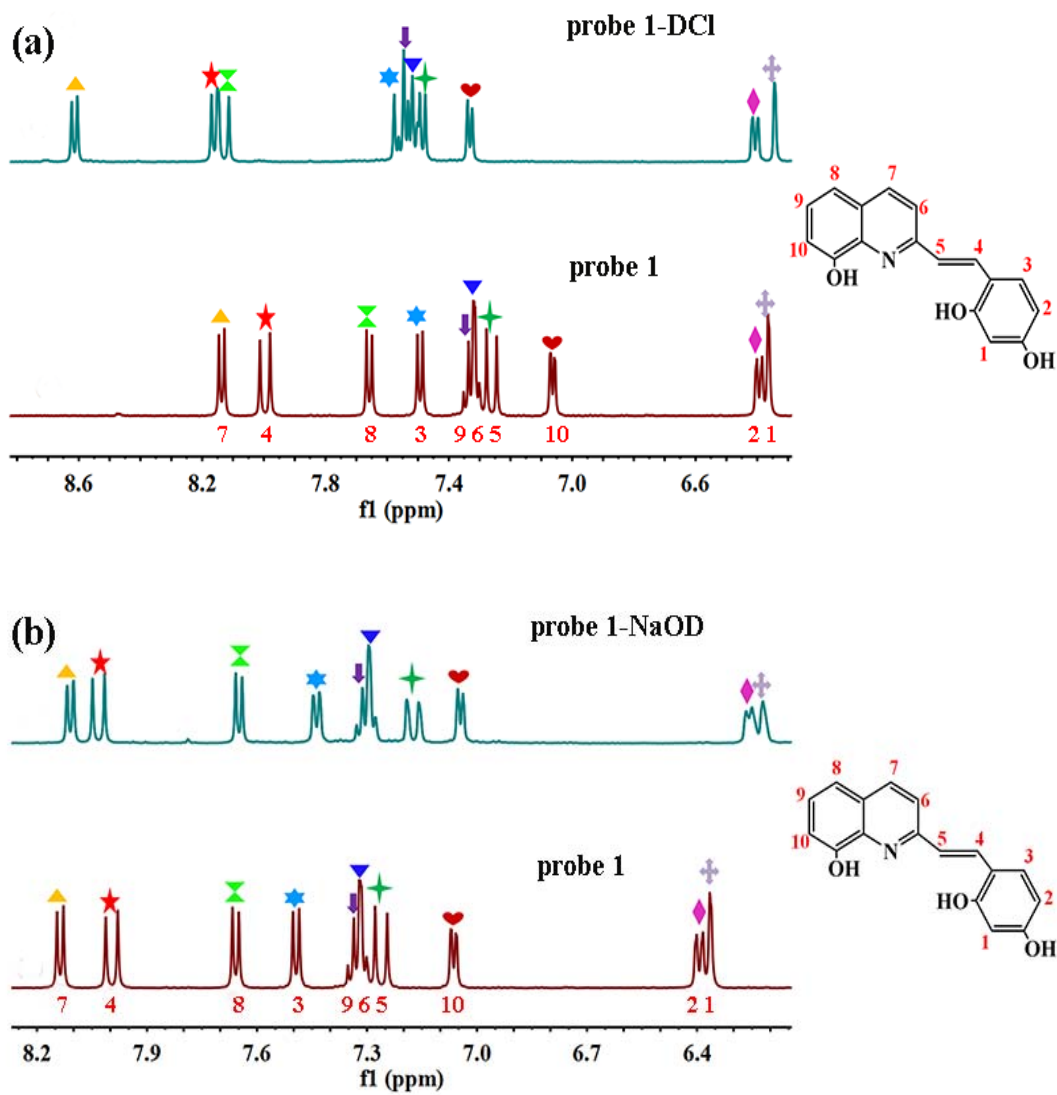
Fig. 8 (a) The ^{1}H NMR spectra of probe **1** (5 mM) and probe **1**-DCl, **(b)** probe **1** (5 mM) and probe **1**-NaOD in CD$_3$CN/D$_2$O (3/1, v/v) at 298 K.

Em: 550 nm

Em: 580 nm

Fluorescence "off"

Fluorescence "on"
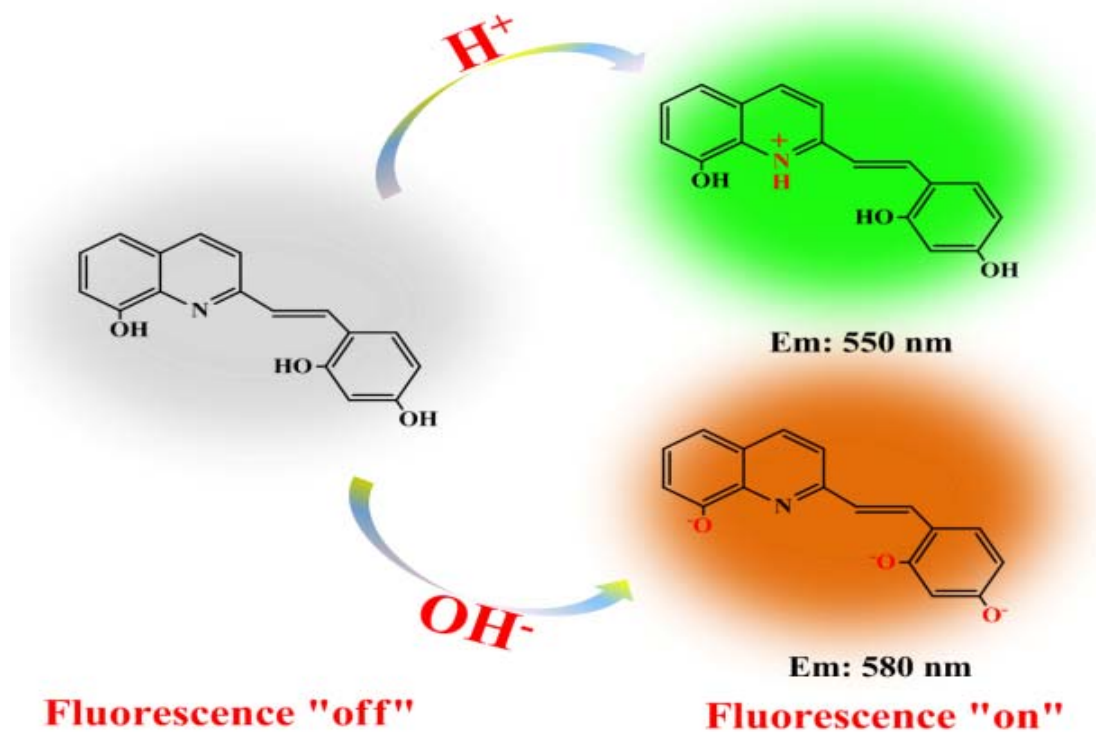
Scheme 2 pH modulated switching of probe **1.**